7074 J. Org. Chem. 1993, 58, 7074–7078

Ab Initio Study of the Potential Energy Surface of the Reaction of Ethylene with Nitronium Ion

Fernando Bernardi,[*,†] Michael A. Robb,[*,‡] Ivan Rossi,[†] and Alessandro Venturini[§]

Dipartimento di Chimica G.Ciamician dell'universita' di Bologna, via Selmi 2, 40126 Bologna, Italy,
Department of Chemistry, King's College London, Strand, London WC2R 2LS, U.K., and Istituto dei
Composti del Carbonio Contenenti Eteroatomi e loro Applicazioni, CNR, Via della Chimica 8,
40064 Ozzano Emilia, Bologna, Italy

Received May 11, 1993[•]

The mechanism of the reaction between ethylene and nitronium ion has been investigated theoretically using SCF, SCF/MP2, QCISD, and MCSCF techniques at the 4-31G and 6-31+G* levels. In addition to the existence and nature of the long-range electrostatic intermediates, reaction paths have been investigated (I) leading to a 1,3 dipolar cycloaddition to yield a five-membered-ring structure, (II) leading to formation of a bridged π complex, (III) leading to formation of a CNO_2 σ-bonded species and subsequently to a CCNO four-membered-ring cycloadduct, and (IV) leading to formation of an intermediate *O*-nitroso form. The 1,3 dipolar cycloaddition is shown to be possible from the electrostatic minimum via a small barrier of 3.4 kcal mol^{-1} at the 6-31+G* QCISD level. At the same computational level, the existence of a bridged π complex, less than 0.5 kcal mol^{-1} above the long-range electrostatic complex, has been demonstrated. The region of the σ-bonded species, which lies 2.8 kcal mol^{-1} higher in energy, is a transition-state region for the formation of a CCNO four-membered ring. The formation of the *O*-nitroso form occurs without any barrier.

1. Introduction

Although electrophilic aromatic nitration has received great attention[1-6] its mechanism has not been completely clarified. This work aims to improve the understanding of the gas-phase mechanism of this important reaction through an ab initio study. Various gas-phase studies[7-10] of aromatic nitration have appeared. It has been shown that the major products of NO_2^+ with benzene, in the gas phase, are nitrogen dioxide (NO_2), the aromatic radical cation $ArH^{\bullet+}$ (70%), and to a lesser extent, an oxygen-containing radical cation $ArHO^{\bullet+}$ (30%).

In this work we shall model the essential aspects of this reaction via a study of the potential energy surface of the reaction between ethylene and nitronium ion. Various ab initio studies[11-13] have already been reported on the ethylene–nitronium ion system. In early work, Bernardi and Hehre[11] located three minima in this potential energy surface at the STO-3G[14] level (see Scheme I): an asymmetric four-membered ring structure (I) and a symmetric five-membered ring structure (II) of nearly equal energy and a bisected nitro form (III) some 60 kcal mol^{-1} less stable. Recently, Borisenko et al.[12] reoptimized these structures with gradient procedures at the SCF 3-21G[15] level (3-21G/3-21G) and also carried out single-point calculations on these optimized structures at the SCF 6-31G*[16] level (6-31G*/3-21G). While structures I and II were characterized as stable energy minima, structure III was found to be a transition structure. Gleghorn and Torossian[13] have confirmed these results at the 6-31G**[17]/4-31G[18] level. Additionally, they have found that the π-complex IV is also a transition state above the nitro form in energy. They have also found at the 4-31G//4-31G level a *O*-nitroso form V at higher energy. They have also shown that introduction of correlation energy at the MP2/4-31G//RHF/4-31G level modifies the previous stability sequence making the π-complex IV lower in energy than the nitro form and the latter more stabilized than the other species.

In this paper we report a theoretical study of the mechanism of the reaction between ethylene and nitronium ion using SCF, SCF/MP2, QCISD, and MC-SCF[19] techniques at the 6-31+G*[20] and 4-31G levels. In addition to the existence and nature of the long-range intermediates, the essential mechanistic questions we shall address relate to reaction paths leading to the following (Scheme I): (I) formation of the four- and five-membered ring structures

---

[†] Universita' di Bologna.

[‡] King's College London.

[§] Istituto dei Composti del Carbonio Contenenti Eteroatomi e loro Applicazioni.

[•] Abstract published in *Advance ACS Abstracts*, October 15, 1993.

(1) Hughes, E. D.; Ingold, C. K.; Reed, R. I. *J. Chem. Soc.* **1950**, 2400.

(2) Ingold, C. K. *Structure and Mechanism in Organic Chemistry*; Cornell University Press: Ithaca, NY, 1953.

(3) (a) Norman, R. O. C.; Taylor R. Electrophilic Substitution in Benzenoid Compounds; Elsevier: New York, 1965. (b) Olah G. A. *Acc. Chem. Res.* **1971**, *4*, 240. (c) Ridd, J. H.; *Ibid.* **1971**, *4*, 248.

(4) Stock, L. M. In *Progress of Physical Organic Chemistry*; Taft R. W., Ed.; Wiley-Interscience: New York, 1976; Vol. 12, Chapter 2.

(5) Olah, G. A.; Narang, S. C.; Olah, J. A.; Lammertsma, K. *Proc. Natl. Acad. Sci. U.S.A.* 1982, *79*, 4487.

(6) Lowry, T. H.; Richardson, K. S. *Mechanism and Theory in Organic Chemistry*, 2nd ed.; Harper & Row: New York, 1981; Section 7.4.

(7) Benezra, S. A.; Hoffmann, M. K.; Bursey, M. M. *J. Am. Chem. Soc.* **1970**, *92*, 7501.

(8) Dunbar, R. C.; Shen, J.; Olah, G. A. *J. Am. Chem. Soc.* **1972**, *94*, 6862.

(9) Ausloos, P.; Lias, S. G. *Int. J. Chem. Kinet.* **1978**, *10*, 657.

(10) Morrison, J. D.; Stanney, K.; Tedder, J. M. *J. Chem. Soc., Perkin Trans. 2* **1981**, 967.

(11) Bernardi, F.; Hehre, W. Y. *J. Am. Chem. Soc.* **1973**, *95*, 3078.

(12) Borisenko, A. A.; Nikulin, A. V.; Wolfe, S.; Zefirov, N. S.; Zyk, N. V. *J. Am. Chem. Soc.* **1984**, *106*, 1074.

(13) Gleghorn, J. T.; Torossian, G. *J. Chem. Soc., Perkin Trans. 2* **1987**, 1303.

(14) Hehre, W. Y.; Stewart, R. F.; Pople, J. A. *J. Chem. Phys.* **1969**, *51*, 2657.

(15) Binkley, J. S.; Pople, J. A.; Hehre, W. Y. *J. Am. Chem. Soc.* **1980**, *102*, 939.

(16) Gordon, M. S.; Binkley, J. S.; Pople, J. A.; Pietro, W. J.; Hehre, W. Y. *J. Am. Chem. Soc.* **1982**, *104*, 5039.

(17) Frisch, M. J.; Pople, J. A.; Binkley, J. S. *J. Chem. Phys.* **1984**, *80* (7), 3265.

(18) Ditchfield, R.; Hehre, W. Y.; Pople, J. A. *J. Chem. Phys.* **1972**, *56*, 2257.

(19) The MC-SCF programs used are those of Gaussian 90 (see ref 22).

(20) Clark, T.; Chandrasekhar, J.; Spitznagel, G. W.; Schleyer, P. v. R. *J. Comput. Chem.* **1983**, *4*, 294.

0022-3263/93/1958-7074$04.00/0

Scheme I

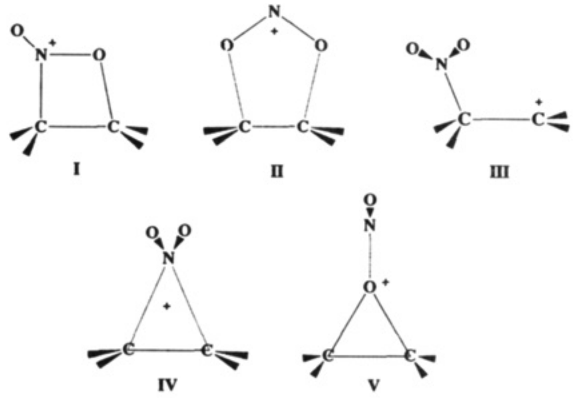

Scheme II

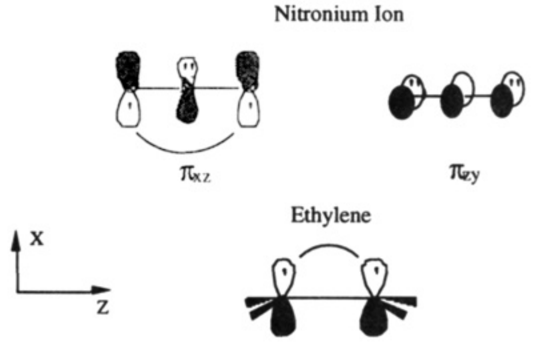

Scheme III

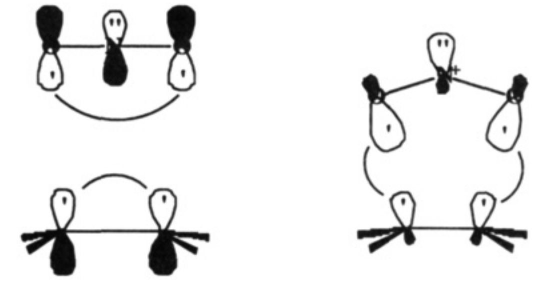

I and II, (II) formation of a σ-bonded species III, (III) formation of a π complex IV, and (IV) formation of an intermediate *O*-nitroso form V.

2. Spin Couplings

The simplest way to visualize the electronic changes involved in the three possible reaction paths is via spin recoupling based upon VB theory. The reactant VB structures are illustrated in Scheme II. The nitronium ion in its ground state is linear, with two orthogonal π systems (π and π' whose occupancies are shown in Scheme II). For the 1,3 dipolar cycloaddition leading to II the spin coupling must change as shown in Scheme III. The reactant bonding situation is characterized by the spin coupling associated with the ground state of the fragments; therefore, ethylene is planar and the nitronium ion is linear. The π system of the nitronium ion involved in this approach is the one denoted as π_{xz} in Scheme II. The product spin coupling involves two triplets coupled to a singlet.[21] The spin recoupling for N attack is summarized in Scheme IV. Again, the overall reactant spin coupling is characterized by the spin coupling associated with the ground state of the fragments. However, in this case the π_{yz} system in Scheme II of the nitronium ion is involved. The product spin coupling involves two radicals, obtained from an electron transfer from the ethylene moiety to the nitronium ion. The two radicals, $NO_2^{\bullet}$ and $H_2CCH_2^{\bullet+}$ couple to form a C–N bond. Thus, the transition region in the reaction involves a charge transfer as opposed to a spin recoupling that occurs in the cycloaddition. The electron transfer will take place in the region of the π complex (structure IV) and will be complete in the products. Finally, the spin recoupling leading to the *O*-nitroso form V is shown in Scheme V. The spin coupling in the product is obtained from an internal electron transfer from the oxygen sp-type lone pair to the nitrogen atom. This will result in subsequent weakening of the O–N bond, due to increased exchange repulsions. The geometry of the excited NO_2^+ state is bent. Since the electron transfer can occur in both orthogonal planes, it follows that in the product spin coupling there are two possible orientations of the NO_2^+ group: perpendicular to the COC plane or in the same plane as COC. Thus we can expect two possible product conformations.

Scheme IV

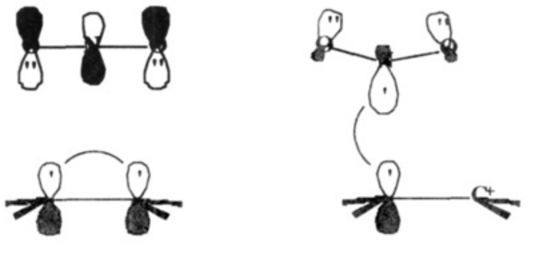

Scheme V

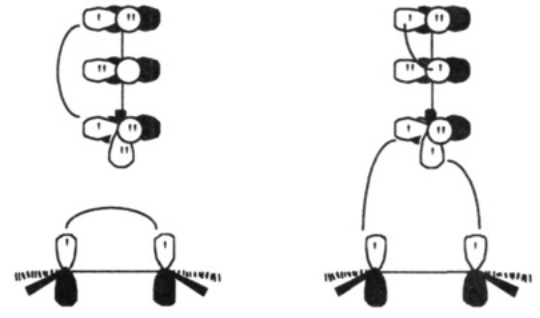

From the preceding qualitative discussion the reaction paths corresponding to 1,3 dipolar cycloaddition reactions to give II involve spin recoupling while reaction paths leading to formation of a σ-bonded species III and then to I, or to formation of a π complex IV, as well to formation of an intermediate *O*-nitroso form V involve charge transfer. However, the formation of the two bonds to give II has been shown to be synchronous; thus, nondynamic correlation (i.e., MC-SCF) is not expected to be important. However, because of the charge-transfer nature involved in the other reaction paths dynamic correlation and basis set considerations will play a deciding role. The inclusion of diffuse and polarization functions in the basis set seems

---

[21] (a) Pross, A.; Shaik, S. S. *Acc. Chem. Res.* **1983**, *16*, 363. (b) Bernardi, F.; Olivucci, M.; Mc Douall, J. J. W.; Robb M. A. *J. Chem. Phys.* **1988**, *89*, 6365. (c) Bernardi, F.; Olivucci, M.; Robb, M. A. *Res. Chem. Interm.* **1989**, *12*, 217.

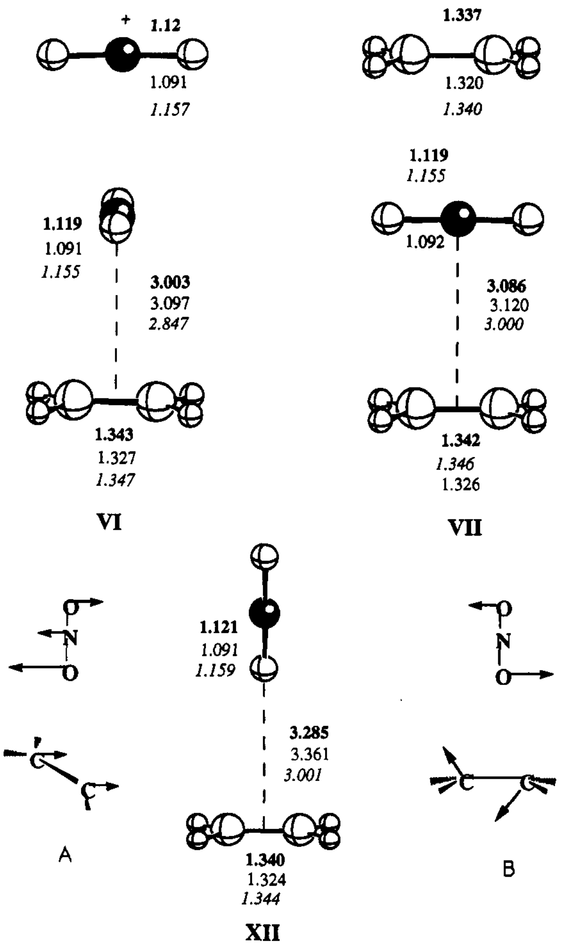

Figure 1. Important geometric parameters for the reactants and the electrostatic structures VI, VII, and XII (MC-SCF results in bold, SCF in plain, and MP2 in italic type). The normal coordinates corresponding to the imaginary frequencies for XII are also shown.

appropriate for obtaining a reliable description of long-range electrostatic complexes and species involving large electron transfers. Thus, SCF and SCF/MP2 at the 6-31+G* level should provide a balanced approach for the study of the potential surface. To obtain accurate energy values, single point calculations have been carried out at the QCISD level. However, it also seems prudent to check the region of the fragmentation transition states using a CAS (complete active space) MC-SCF approach.[19] In CAS-SCF computations, the only element that is somewhat subjective is the choice of the active orbital space (i.e., those orbitals that may have variable occupancy). In the present case, the orbitals that should be included in the valence space, in order to describe correctly all various types of attack of the nitronium ion on ethylene are the π orbitals of the two reactants, i.e., the two sets of allylic-type orbitals of NO_2^+ and the π system of ethylene. Such a valence space consists of eight orbitals/10 electrons. However, the two lowest energy orbitals of the allylic systems were found to have orbital occupancies which approach 2. So the active space can be reduced in dimension to six orbitals/six electrons without changing the energy.

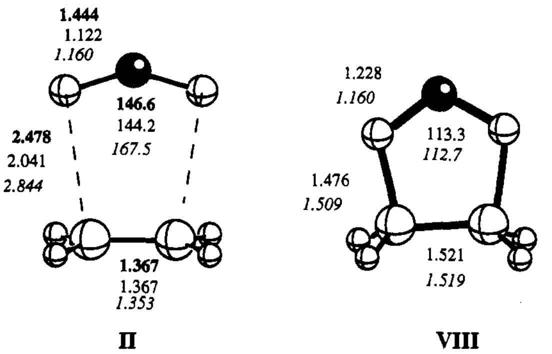

Figure 2. Relevant structural parameters of the transition state II and of the minimum VIII found for the 1,3 dipolar cycloaddition pathway (MC-SCF results in bold, SCF in plain, and MP2 in italic type).

All computations were performed using the Gaussian 90[22] suite of programs.

3. Results and Discussion

The mechanistic aspects of the addition of the nitronium ion to ethylene involve consideration of the following: (1) the nature of the long-range electrostatic intermediate, (2) a 1,3 dipolar-type reaction path leading to the formation of the five-membered ring structure II, (3) the reaction path to formation of a σ-bonded species III, (4) the reaction path leading to formation of a π complex IV, (5) the reaction path leading to formation of the four-membered ring I, and (6) the reaction path leading to formation of an intermediate *O*-nitroso form V. Clearly, 3–5 are closely related.

We begin our discussion by considering the long-range electrostatic complexes (see Figure 1). In this region we have found three critical points, which have been fully optimized with gradient and characterized through the computation of the analytical Hessian matrices. The geometry optimization and characterization have been carried out at the 4-31G CAS MC-SCF, 6-31+G* SCF, and 6-31+G* MP2 levels. Furthermore, we have carried out single point computations at the 6-31+G* QCISD level using the MP2-optimized geometry. Structure VI is a minimum and lies 7 (MC-SCF), 8.6 (SCF), 11 (MP2), and 10.5 (QCISD) kcal mol^{-1} below the isolated reactants. At the SCF/MP2 level, the region of the electrostatic complex is very flat, and at this level we have been able to optimize structure VI with a maximum force of the order of 0.001 (expected error in the interfragment distance is of the order of 0.1 Å). Twisting the NO_2^+ group leads to a transition state (structure VII) that has a barrier of 0.7 kcal mol^{-1} at the SCF/MP2 level. We have also characterized an electrostatic complex with the structure shown as XII. This structure, which lies 4.9 kcal mol^{-1} above structure VI at the SCF/MP2 level, has two imaginary frequencies. The corresponding normal coordinates (shown as arrows in Figure 1) are directed at the *O*-nitroso structure V (Scheme I). Thus, the only true minimum in the region of the electrostatic complex is VI. In all the electrostatic complexes the geometries of the two fragments are almost unmodified.

The optimized geometries for the 1,3 dipolar-type attack are collected in Figure 2, and the energetic can be found in Table I. In the transition state II the MC-SCF value of the CN and NO distances are longer than the corresponding values computed at SCF level. The SCF and

---

[22] Gaussian 90: Frisch, M. J.; Head-Gordon, M.; Trucks, G. W.; Foresman, J. B.; Schlegel, H. B.; Raghavachari, K.; Robb, M. A.; Binkley, J. S.; Gonzalez, C.; Defrees, D. J.; Fox, D. J.; Whiteside, R. A.; Seeger, R.; Melius, C. F.; Baker, J.; Martin, R. L.; Kahn, L. R.; Stewart, J. J. P.; Topiol, S.; Pople, J. A. Gaussian, Inc., Pittsburgh, PA.

Table I. Energy Values E_h of Reactants and of the Various Critical Points[a]

	4-31G MC-SCF	6-31+G* SCF	6-31+G* SCF/MP2	6-31+G* QCISD
reactants	−281.83696	−281.71826	−282.53758	−282.53446
VI	−281.84818 (M)	−281.73190 (M)	−282.55504[b] (M)	−282.55114
VII	−281.84786 (TS)	−281.73129 (TS)	−282.55394 (TS)	
II	−281.82109 (TS)	−281.70278 (TS)	−282.55353 (TS)	−282.54576
VIII		−281.83116 (M)	−282.60483 (M)	
IV	−281.81904 (M)	−281.72061 (TS)	−282.55823 (M)	−282.55032
III		−281.73090 (SOSP)	Not existent.	
IX		−281.74209 (TS)	−282.52346 (TS)	
X		−281.74802 (M)	−282.52799 (TS)	
XI		−281.74400 (TS)	−282.52363 (TS)	−282.54668
I		−281.80875 (M)	−282.59628 (M)	
XII	−281.84259 (SOSP)	−281.72424 (SOSP)	−282.54725 (SOSP)	
V		−281.82434 (TS)	−282.61317 (M)	
XIII		−281.82482 (M)	−282.60735 (TS)	

[a] M = minimum, TS = transition state, SOSP = second-order saddle point. [b] Maximum force on the order of 0.001.

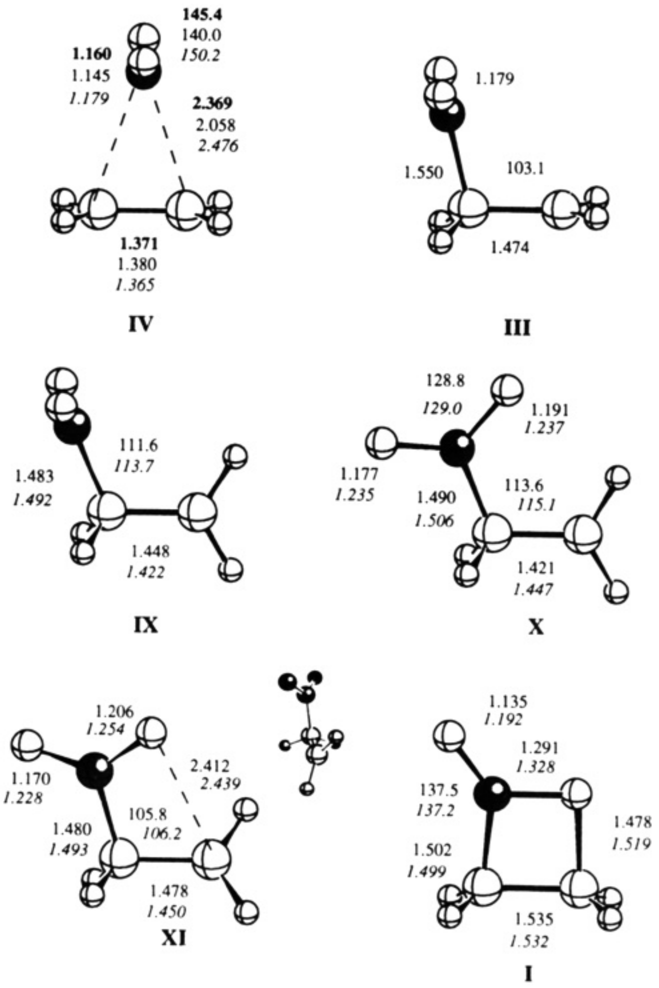

Figure 3. Geometric parameters of the structures found for reaction path corresponding to the formation of a σ-bonded species III to formation of a π complex IV and to formation of the four-membered ring I (MC-SCF results in bold, SCF in plain, and MP2 in italic type).

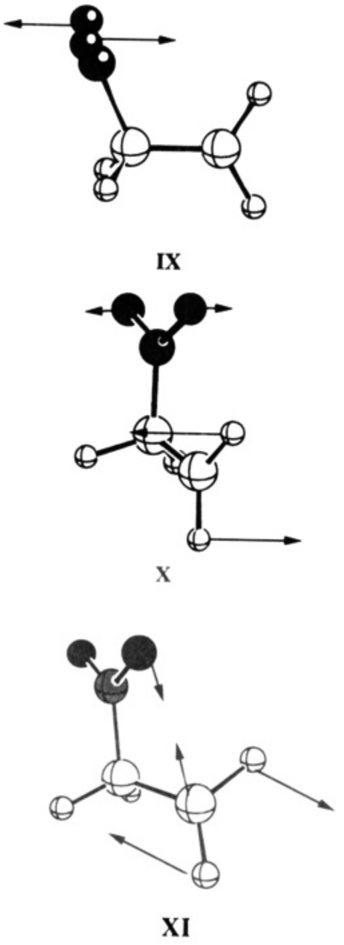

Figure 4. Normal coordinates corresponding to imaginary frequencies of the structures IX, X, and XI computed at the MP2/6-31+G* level.

MC-SCF energy barriers along this pathway are very similar as expected, i.e., 17 kcal mol^{-1} at the SCF and 18.3 kcal mol^{-1} at the MC-SCF level. However dynamic correlation has a large effect: at the SCF/MP2 level the CN distances are much longer and the barrier from the electrostatic minimum almost disappears (around 0.5 kcal mol^{-1}).

Now we turn our attention to the related reaction paths corresponding to formation of a π complex IV and to formation of a σ-bonded species III, which leads ultimately to formation of the four-membered ring I. The structural information is collected in Figure 3. We shall consider the π complex IV first. At MC-SCF and SCF/MP2 levels this structure is a minimum that lies just above (0.5 kcal mol^{-1} at QCISD level) the electrostatic complex. While the structural parameters at the MC-SCF and SCF/MP2 levels are in good agreement, dynamic correlation (MP2) is necessary to obtain reliable energetics. The structures for a σ-bonded species (III, IX, X, XI, and I) are also included in Figure 3. The surface at the SCF/MP2 level is completely flat. Structures III, IX, X, and XI all lie in

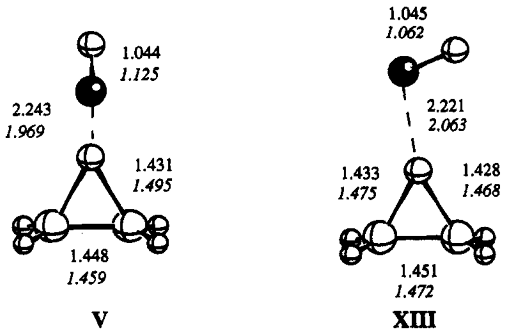

Figure 5. Geometric parameters of the *O*-nitroso forms V and XIII (SCF results in plain and MP2 in italic type).

a range of 2.8 kcal mol^{-1} of each other at the SCF/MP2 level, and the lowest energy structure X lies 19 kcal mol above the π complex IV. To improve the accuracy of the energetic description, we have carried out single point computations of structures IV and XI at the 6-31+G* QCISD level using the 6-31+G*/MP2 optimized geometry. At this level the surface becomes even more flat. The energy difference between IV and XI is 21.7 kcal mol^{-1} at the SCF/MP2 level and 2.3 kcal mol^{-1} at the QCISD level.

The four-membered ring complex lies in a well-defined minimum that lies 36.8 kcal mol^{-1} below the reactants. The nature of the σ-bonded species (III, IX, X, and XI) must be regarded as ambiguous because they lie so close together in energy and differ only in minor conformational changes. However, XI is a well-defined transition state at the SCF/MP2 level for the formation of I (see normal coordinate plotted in Figure 4). Thus, the region of σ-bonded species XI corresponds to a transition state region between a well-defined π complex IV that is accessible from the electrostatic minimum VI with almost no barrier and the four-membered ring I. The charge transfer is very large in the π complex IV and is complete in the products.

Finally, we turn our attention to the reaction path leading to formation of an intermediate *O*-nitroso form V. The structural information is given in Figure 5. The electrostatic critical point for O attack (Figure 1, XII) has two imaginary frequencies. Thus, O attack will avoid this region. In spite of extensive searches at the MC-SCF and SCF/MP2 levels, we could find no transition state for O attack. Rather, we can find only structures in the product region (Figure 5, V and XIII) corresponding to an *O*-nitroso form with one NO bond partly broken. At the SCF/MP2 level, these two structures differ in energy by 3.6 kcal mol^{-1} and structure V is a minimum and XIII is a transition structure connecting two equivalent forms of V. The *O*-nitroso structure V lies 47.4 kcal mol^{-1} below the reactants at SCF/MP2 level.

4. Conclusions

In this paper we have investigated theoretically the mechanism of the reaction between ethylene and nitronium ion using ab initio MC-SCF, MP2/SCF, QCISD, and SCF techniques as a model for electrophilic aromatic substitution. The 1,3 dipolar cycloaddition is possible from the electrostatic minimum via a small barrier of 3.4 kcal mol^{-1} at the QCISD level. The existence of a bridged π complex is demonstrated for this model system. This bridged π complex lies less than 0.5 kcal mol^{-1} above the long-range electrostatic complex at the QCISD level. The region of a σ-bonded species lies 19.7 kcal mol^{-1} lower in energy at the MP2 level and is a transition state region for the formation of a CCNO four-membered-ring. The energetics of the σ-bonded species is very sensitive to the inclusion of dynamic electron correlation. The formation of the *O*-nitroso form occurs without any barrier. These results are in agreement with the experimental evidence[7] obtained for the gas-phase interaction of NO_2^+ with benzene where the product is an oxygen-containing radical cation, most likely obtained from the decomposition of a nitroso form.